Egyptian Journal of Chemistry

http://ejchem.journals.ekb.eg/

Removal of dyes from aqueous solution using zinc terephthalic acid metal-organic frameworks (Zn-TPA-MOF) based adsorbent

Mohamed Saeed Iprahim [1] Rabie Saad Farag [2] Hesham Ramzy Tantawe [3]

[1] Armed forces / Al-Azhar university

[2] Egypt

[3] Military Technical College

Abstract

Zinc (II)-terephthalic acid metal-organic framework (Zn-TPA-MOF) was synthesized by a solvothermal method and characterized by Scanning Electron Microscope/Energy Dispersive X-Ray (SEM/EDX), Fourier Transformer Infrared (FTIR), Raman, and X-ray diffraction (XRD). Raman microscopy and XRD expose that terephthalic acid (TPA) acts as a bidentate ligand towards zinc(II) through the two carboxylate groups. FTIR and Raman microscopy emphasize the formation of coordination bonds between the electron-acceptor Zn(II) atoms and the electron-donor oxygen atoms. SEM shows that the (Zn-TPA-MOF) has a bar-like macro-structure with small dimensions, e.g., 200 nm. (Zn-TPA-MOF) the structure is proposed to be a cationic metal-organic framework and extremely water-stable. Due to these features, (Zn-TPA-MOF) was studied for the Removal of cationic and anionic dyes, using synthetic cationic dye as Methylene Blue (MB^+) and an anionic dye as Congo Red ($C.R^-$) in an aqueous solution. Zn-TPA-MOF has a strong adsorption potential for both C.R. and M.B. due to the maximum adsorption capacity of C.R. (769.23 mg/g) and MB (147.06 mg/g) onto Zn-TPA-MOF.

Keywords: Ligand; Metal-organic framework; Zinc(II)-Terephthalic (Zn-TPh MOF)

1- Introduction

As industrialization, urbanization, and human habitations continue to grow rapidly, water bodies around the world are at risk of pollution [1-2]. More than 10,000 tons of dyes are used by textile industries worldwide each year, with approximately 5000 tons of these dyes and 3600 tons of different wastes containing high concentrations of dyes being discharged into water streams [3-4]. These industries' effluents contain high levels of synthetic dyes, which are destructive to the environment [5]. Many dyes found in industrial wastewater are harmful, carcinogenic, and genotoxic [6]. To remove dyes from industrial effluents, various technologies have been used, including adsorption, coagulation, advanced oxidation, and membrane separation [7]. Because of its ease of use and high efficiency, adsorption is considered one of the most effective advanced wastewater treatments for removing hazardous inorganic and organic pollutants in effluents [8-11]. Porous materials have received attention from researchers in their quest to develop more effective adsorbents [12]. One such porous adsorbent is metal-organic frameworks (MOF).

Metal-organic frameworks (MOFs) are crystalline three-dimensional porous materials formed by bond coordination from multifunctional ligands and metal ion species [13]. MOFs have a wide range of configuration and construction options, high thermal and mechanical stability, tunable pore properties, a large surface area, and reworkable metal sites. These properties have recently enabled the use of MOFs in catalysis [14-16], gas recovery and storage[17-18], substance separation and adsorption [19], and nanomaterials [20]. Prominent among these applications of MOFs is the detection and adsorption of pollutants. MOFs have been used as adsorbents for organic contaminants in liquid-phase extractions [21-23], solid-phase extractions [24-25], solid-phase micro-extractions [26-27], high-performance liquid chromatography [28-29], pre-concentration and detection of metal ions [30].

Here, the purpose of this study was to simply comprehend and investigate the facile synthesis of

*Corresponding author e-mail: errmohammed123@gmail.com; (Mohamed Saeed Iprahim).

Received date 05 January 2022; revised date 28 January 2022; accepted date 31 January 2022

DOI: 10.21608/ejchem.2022.114894.5218

Zn-TPA-MOF. To assist the production of Zn-TPA-MOF, solvothermal process was used followed by its characterization using SEM/EDX, FTIR, Raman and X-ray diffraction. Additionally, The adsorption of congo red (CR) and methylene blue (MB) onto Zn-TPA-MOF was investigated in respect of isotherms to determine the superior adsorbent.

2- Experimental

2.1 Synthesis

The prime chemicals utilized for the preparation of the desired zinc-terephthalate metal-organic framework (Zn-TPh) were Zinc (II), nitrate hexahydrate (98 %, Sigma-Aldrich), and 1,4 dicarboxylic acid (98%, Sigma-Aldrich). N, N-dimethyl formamide (DMF) (99.8%, Sigma-Aldrich) was selected as solvent and reaction medium. Absolute ethanol (99.9%, Fisher Scientific) was used to wash during all synthesis steps. Regarding preparation producers, a stoichiometric ratio was maintained between the reactants. Typically, 0.01 mole of terephthalic acid (TPA) and 0.01-mole zinc nitrate hexahydrate were completely dissolved in 100 ml of DMF after mixing for 30 min with magnetic steering. The obtained solution was transferred to a 200 ml perfectly sealed Teflon tube and then subjected to hydrothermal heating in an oven at 120ºC for 18 h. The obtained white crystals product was washed three times by DMF and three times by absolute ethanol. Finally, the washed product was dried at 80ºC for 24 h [31].

2.2 Instrumentation

The surface morphology of the synthesized Zn-TPA-MOF was investigated using SEM (EVO-MA10, ZEISS) and TEM (JEM-2100F, JEOL, Japan). Elemental composition was analyzed by energy-dispersive X-ray (EDX) coupled with Scanning Electron Microscopy (SEM) device. Moreover, Raman spectroscopic measurements were performed using a dispersive Raman microscope (Bruker, Germany, model Senterra II). The objective (Nikon 20×) was used to focus the Raman excitation source (10 mW, 532 nm neodymium-doped yttrium aluminum garnet (Nd: YAG) laser- Bruker, Germany). Further, FTIR analysis was achieved via the standard KBr pellet method on Perkin Elmer Spectrum One FTIR spectrometer, USA. The conformable spectra were tested between 500 and 3500 cm^{-1}. Furthermore, the crystalline structure was inspected using XRD (XRD, D8 Advance, Bruker Corporation, Germany), using a copper tube (Cu Kα) and wavelength (λ) of 0.15419 nm at a speed of scanning 1 degree/min and sample angle interval of 0.03 degree. The surface area of the samples was measured by using the BET (NOVA Station A) instrument. The efficiency removal of dyes can be measured using a U.V. spectrophotometer (HACH double beam model DR-5000) at (λ) 496 nm for C.R. and 664 nm for MB [32].

2.3. Adsorption experiment

The adsorption efficiency can be determined using a Glas-col agitator (USA) under various conditions such as contact time (0–60 min), rate of shake (400 rpm), pH of dye solution (4–10), adsorbent amount, Zn-TPA-MOF (30 – 60 mg/L), Congo red (C.R.) concentration (20–50 ppm) and Methylene blue (M.B.) concentration (1–7 ppm), temperature (25°C), and a definite volume of (100 mL).

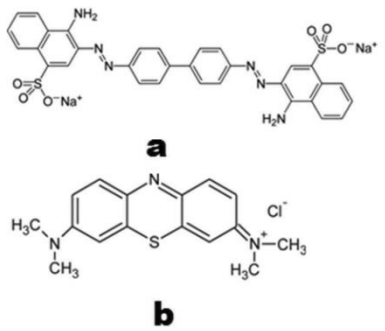

Fig.(1): Structure of (a) CR and (b) MB

(100 mL) dye was transferred to a series conical flask holding the adsorbent dosage. We used a (0.1 M) solution of HCl or NaOH to alter the pH of the dye solutions at the start. After every 10 minutes, remove 1 ml of the suspension adsorbent solution and centrifuge for 5 minutes. Then measure the absorbance with a U.V. spectrophotometer at wavelengths of 496 nm for C.R. and 664 nm for M.B. Using the following equation to calculate the reduction percentage (percent) [33, 34].

$$\text{Removal} = \frac{C_o - C_e}{C_o} \times 100 \qquad (1)$$

where $C_\circ$ is the initial concentration of dyes (mg/L) and C_e is the concentration of dye (mg/L) at equilibrium. The amount of the pollutant retained in the MOFs at equilibrium, q_e (mg/g), can be calculated by the following equation [34]:

$$q_e = \frac{V}{m}(C_o - C_e) \qquad (2)$$

where V is the volume of tested solution (L), m is the mass of Zn-TPA-MOF used (g).

3- Result and Discussion

3.1 *Characterization of the synthesized* MOF

3.1.1 FT-IR and Raman characterization

In Fig.(2) is presented the material was compared with terephthalic acid which most important bands are found in 3062 and 1672 cm^{-1}, these are attributed to the bonds O–H and C=O,

respectively. On the other hand, in the FT-IR spectra, displacement of the band in 1672.0 cm^{-1} to 1587 cm^{-1} is observed, which is attributed to the formation of a coordination bond C–O–Zn [35]. In wavenumbers higher to 3000 cm^{-1} is possible to observe a signal attributed to water molecules.

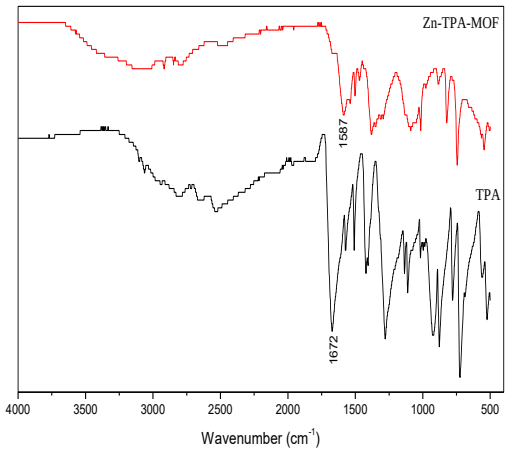

Fig.(2): Zn-TPA-MOF characterization by FT-IR

Raman spectra were recorded for Zn-TPA-MOF. As shown in Fig.(3), five strong Raman bands were observed at 630, 862.5, 1134, 1429.5, and 1611 cm^{-1} for Zn-TPA-MOF, which are consistent with the results reported by Bordiga et al.[36]. Those bands are associated with organic benzene rings and vibration modes of carboxylate groups [37].

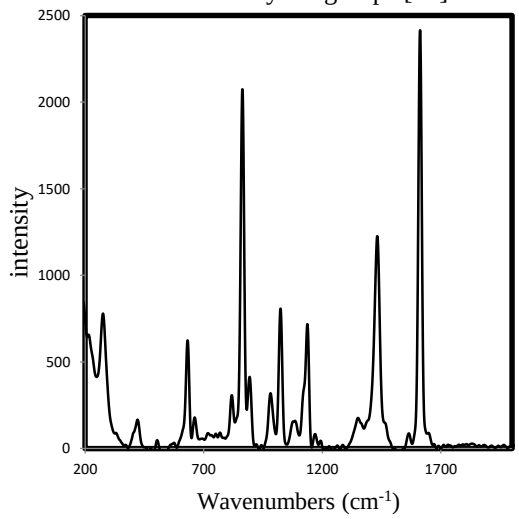

Fig.(3): Raman characterization of Zn-TPA-MOF

3.1.2 XRD characterization

The observed X-ray Diffraction pattern of the Zn-TPA-MOF is shown in Fig.(4). The X-ray diffraction pattern illustrates the monoclinic phase of the Zn-TPA-MOF. The XRD pattern shows a clear peak around 2θ values ~ 9.74º, 11.66º, 14.66º, 19.26º and 19.66º. The strong XRD intensity at 9.74° demonstrates that many crystal faces at (220) were formed in the Zn–TPA–MOF.

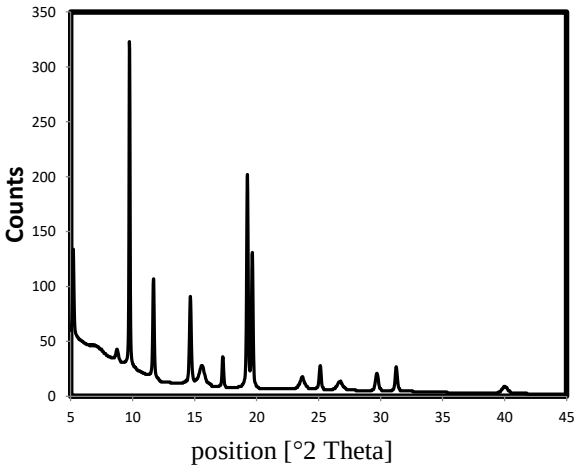

Fig.(4) XRD pattern of Zn-TPA-MOF

3.1.3 SEM/EDX characterization

These results are consistent with the SEM characterization shown in Fig.(5a). The lack of some crystal faces indicates that the morphology of Zn-TPA-MOF is a random slab of a certain thickness rather than a cubic crystal. The Zn-TPA-MOF is probably an impure crystal phase with an irregular shape, as shown in the SEM photo. This may be caused by the multiple coordination modes in the Zn-MOF crystals that formed the multiple structures. Fig.(5b) shows regular cubic morphology and large crystallite size.

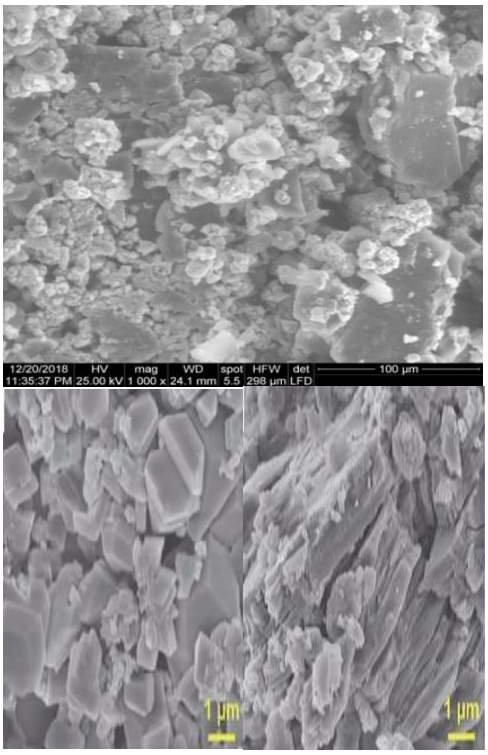

(a)

(b)

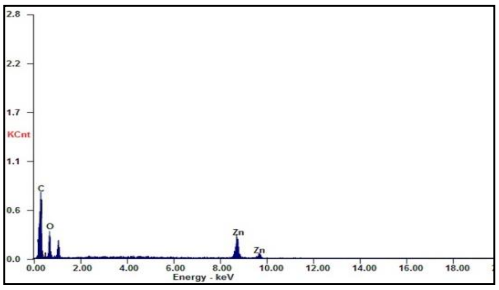

(c)

Fig.(5) SEM images (a,b) and EDX spectra (c) of Zn-TPA-MOF

From all the previous characterization, Figure (6) shows the structure of Zn-TPA-MOF

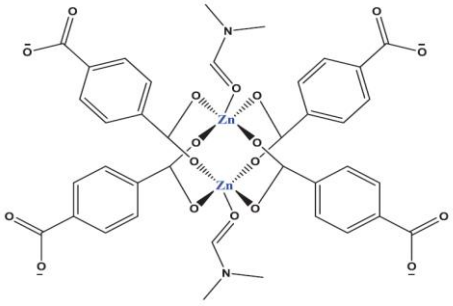

Fig.(6): Structure of Zn-TPA-MOF

3.2 Dyes uptake and adsorption study

3.2.1 Effect of contact time

Contact time is a key operational parameter determining the volume and space required for sorption units. Investigation of contact time, therefore, comprises a crucial part of a sorption study that gives insight into the economy of the process. Fig.(7) shows the C.R. removal percentage by agitation time from 10 to 60 min. The figure shows a significant adsorption improvement from about 32.7% to 87.07% by increasing mixing time within the range studied. This incremental adsorption efficiency by contact time could be attributed to the high availability of sorption sites.

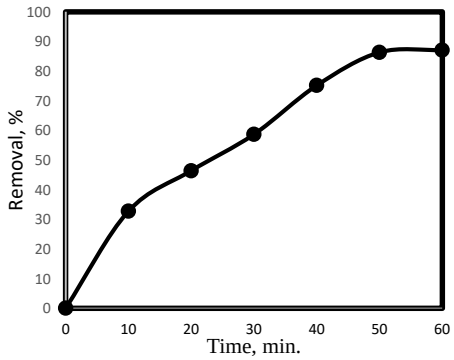

Fig.(7): Effect of contact time on CR adsorption (C_o = 40 mg/L; adsorbent dose: 60 mg/L; pH = 6; Temperature = 25°C)

Fig.(8) shows the M.B. removal percentage by agitation time from 10 to 60 min. The figure shows a significant adsorption improvement from about 51.24% to 95.64% by increasing mixing time within the range studied.

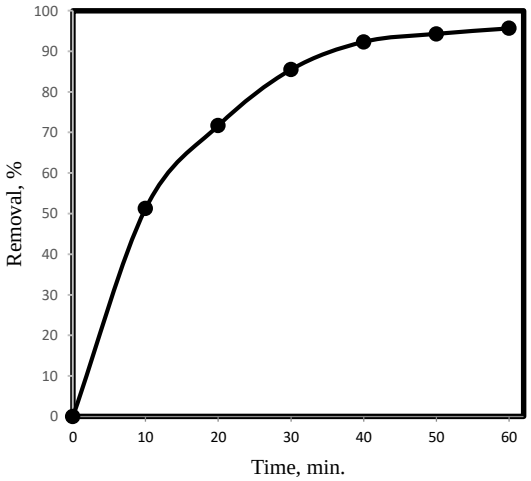

Fig.(8): Effect of contact time on MB adsorption (C_o = 5 mg/L; adsorbent dose: 60 mg/L; pH = 10; Temperature = 25°C)

3.2.2 Effect of adsorbent dose

Knowing the Effect of adsorbent mass and solute concentration is imperative in a sorption study. The Effect of the adsorbent dose was studied by varying the mass of the adsorbent in the range 30–60 mg/L. Figs.(9&10) show C.R. and M.B. adsorption percentage increased considerably when higher adsorbent doses were applied to the solution. This is due to the higher accessible sorption sites at elevated adsorbent mass.

Fig.(9) shows the variation of removal efficiency of Zn-TPA-MOF with different loading concerning fixed C.R. initial concentration of 40 ppm and pH 6 at 25°C. Obviously, increased loading of Zn-TPA-MOF from 30 to 60 mg/L led to increasing removal performance. The maximum Removal reaches 87.07% for 60 mg/L. Similarly, Fig.(10) shows the change of removal efficiency of 5 mg/L M.B. as initial concentration using different amounts of Zn-TPA-MOF. Obviously, increased loading of Zn-TPA-MOF from 30 to 60 mg/L led to increasing removal performance. The maximum successful Removal reaches 95.64% for 60 mg/L loading after 60 min.

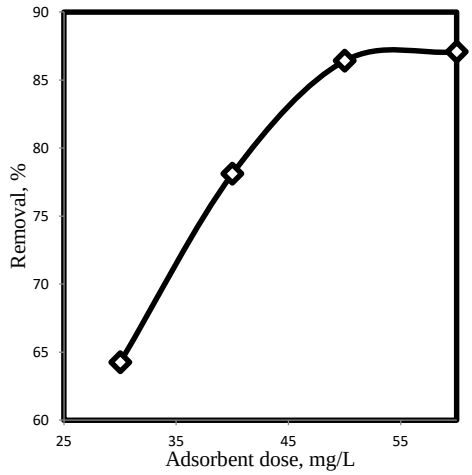

Fig.(9) Effect of dose of Zn-TPA-MOF on adsorption of C.R. dye (Time of contact = 60 min.; C_o = 40 ppm, pH = 6; Temp., 25°C)

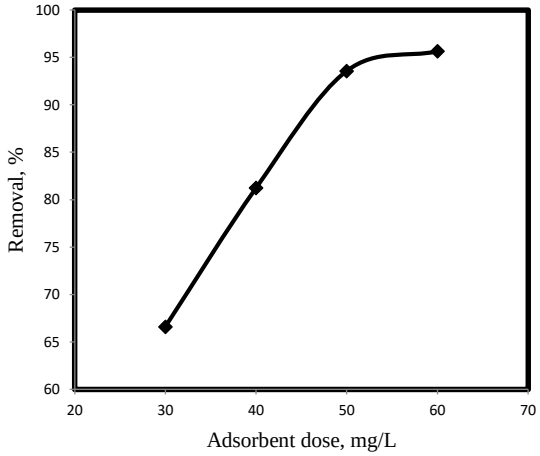

Fig.(10) Effect of dose of Zn-TPA-MOF on adsorption of M.B. dye (Time of contact = 60 min.; C_o = 5 ppm, pH = 10; Temp., 25°C)

3.2.3 Influence of pH

The Effect of pH on adsorption removal effectiveness is critical for scaling up Zn-TPA-MOF use and explaining any pH restrictions for future applications.

A variety of pH values were evaluated, covering the pH range of 4 to 12. The primary goal of studying Zn-TPA-MOF adsorption within the chosen pH range is to confirm the possibility of using the complete industrial waste pH range.

Figures 11 and 12 show the influence of pH on the adsorption deactivation curves of 40 ppm C.R. and 5 ppm MB by 50 mg/L Zn-TPA-MOF at 25°C. pH had a significant influence on adsorption efficiency, which ranged between 62.27% and 86.41% in the case of C.R. and 38.8% and 93.52% in the case of M.B. across the pH range studied.

The adsorption effectiveness of C.R. is weak in more acidic and basic media, although it reaches neutral media. At pH 4, the efficiency is 79.65%, and at pH 10, it is 62.27%, while at pH 6, it is 86.41%. At pH 6, the system's maximum C.R. elimination was attained, which could be related to a relative rise in H^+ ion levels in the system at higher pH values (Fig.11).

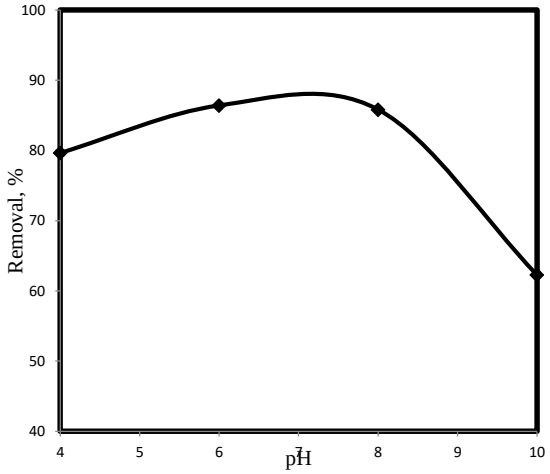

Fig.(11) Effect of pH on removal profile of C.R. by Zn-TPA-MOF (C_o : 40 ppm ; adsorbent dose: 50 mg/L; contact Time: 60 min.; temperature 25°C.

When MB is dissolved in water, it produces positive charge ions. In acidic media, the positively charged surface of the MOF as sorbent reduces the M.B. adsorbate's adsorption. The electrostatic attraction between the positive charge of the M.B. dye and the negative charge of the Zn-TPA-MOF as adsorbent increases when the pH of the M.B. solution is raised, resulting in increased adsorption removal of M.B. The adsorption efficiency of Zn-TPA-MOF is 38.8% at pH 4, 46.99 % at pH 6, and 49.38 % at pH 8, and 93.57% at pH 10. At pH 10, the most effective elimination of M.B. was achieved (Fig.12).

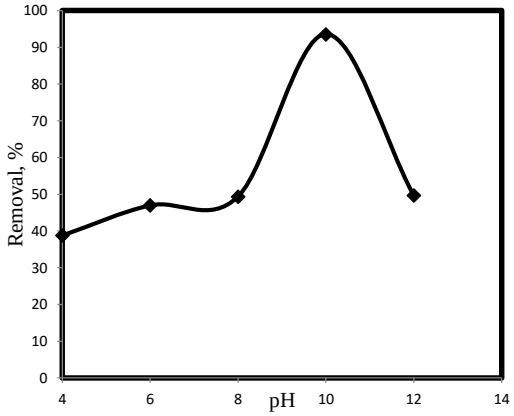

Fig. (12) Effect of pH on Removal of M.B. by Zn-TPA-MOF (C_o : 5 ppm ; adsorbent dose: 50 mg/L; contact Time: 60 min.; temperature 25°C).

Figure 13 depicts the solution's final pH values for all initial pH values employed, which were

approached to the specified pH of 6.39. After 24 hours of dipping the Zn-TPA-MOF in several pH solutions, the same value was detected at equilibrium. The more practical pH value was found to be about pH 6 during the catalytic process, that is, the first 2.5 hours. The initial pH values for the blank solution (without Zn-TPA-MOF) remained stable till the end of the tests. As a result, changing the initial pH values after Zn-TPA-MOF immersion to a constant value causes the response to the initial pH values to be mostly related to the Effect of Zn-TPA-MOF without any involvement from the dyes. The buffering behavior of Zn-TPA-MOF is reflected by the pH 6.39, which can be referred to as pHpzc. On the other hand, traditional semiconductors preserve the acidity or basicity of the treated solutions while displaying a positively or negatively charged surface.

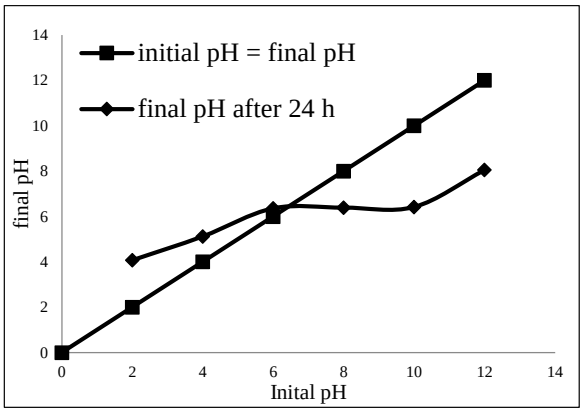

Fig.(13) Determination of pH_{PZC} (Final pH vs. Initial pH) of Zn-TPA-MOF.

3.2.4 Effect of the initial concentration of dyes

Using varied concentrations of C.R. and M.B., the Effect of the initial dye concentration on the removal process was investigated. Initial concentration of C.R. dye ranged from (30 to 50) ppm at pH 6 and (1 to 7) ppm at pH 10 for M.B. dye. The amount of Zn-TPA-MOF was set at 50 mg/L at temperature 25°C. The Effect of initial C.R. and M.B. concentration under the optimum condition was investigated and the results presented in Figs.14 & 15. As the figure shows, the C.R. removal percentage decreased sharply from ~ 98.15% to ~ 66.94% by increasing C.R. concentration from 20 to 50 mg/L. The limited sorption sites of Zn-TPA-MOF under a constant dose, led to a significant loss of adsorption efficiency at elevated C.R. concentration.

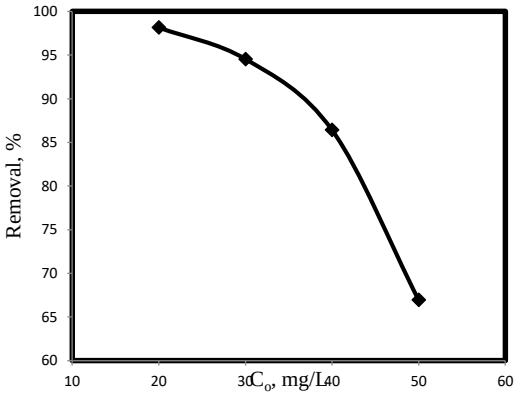

Fig.(14) The effect of initial C.R. concentration on removal efficiency under the optimum condition (pH 6, contact time 60 min, adsorbent dosage 50 mg/L).

In the case of M.B., the concentration range under investigation was 1 to 7 ppm. The elimination efficiency remained consistent at 97.85-93.57 percent as the M.B. dye concentration increased from 1 to 5 ppm. However, when the M.B. dye concentration approaches 7 ppm, the removal efficiency drops to 89.02%.

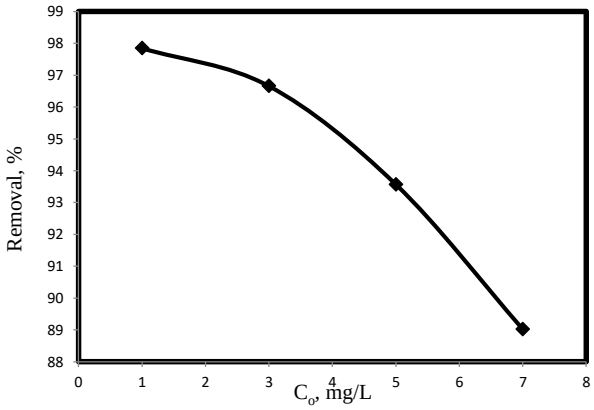

Fig.(15) The effect of initial M.B. concentration on removal efficiency under the optimum condition (pH 10, contact time 60 min, adsorbent dosage 50 mg/L).

3.2.5 Adsorption Isotherms

Equilibrium isotherm data were analyzed using Langmuir and Freundlich isotherm models. The Langmuir isotherm model is based on the adsorption of the monolayer of dye molecules onto a surface of the Zn-TPA-MOF. The linear form of the Langmuir adsorption model is represented as [38]:

$$\frac{C_e}{q_e} = \frac{1}{Q_m} C_e + \frac{1}{bQ_m} \quad (3)$$

Where C_e is the equilibrium concentration of dye (mg/L), q_e is the equilibrium adsorption capacity (mg/g), Q_m (mg/g), and b (L/mg) are the maximum adsorption capacity and binding constant, respectively. The parameters of the Langmuir model are listed in Table 1.

The Freundlich isotherm model is an empirical equation that refers to a heterogeneous adsorption system. The Freundlich isotherm model is shown by the following equation [39]:

$$log\ q_e = \frac{1}{n}\ log\ C_e + log\ K_F \qquad (4)$$

Where q is the equilibrium adsorption capacity (mg/g), *Ce* is the equilibrium concentration of dye (m/L), *K.F.* and *1/n* are the Freundlich constants for the adsorption capacity (mg/L) and a measurement of efficiency of adsorption, respectively. The values of *K.F.* and *1/n* were calculated and collected in Table 1.

3.2.5.1 Adsorption Isotherms of C.R. dye on Zn-TPA-MOF

According to the Langmuir model, maximum adsorption corresponds to a saturated monolayer of C.R. dye molecules on the adsorbent surface. The Langmuir monolayer adsorption capacity was estimated and found to be 769.23 mg/g. Specific adsorption (C_e/q_e) against equilibrium concentration $(1/C_e)$ in a linear plot (Fig.16) with a correlation coefficient of 0.9997. (Table 1). (Figure 16)

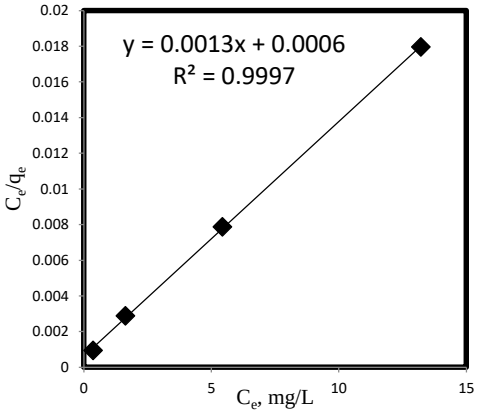

Fig.(16) Langmuir isotherm for C.R. adsorption on Zn-TPA-MOF.

The Freundlich model is often used to represent heterogeneous systems. The Freundlich parameter 1/n = 0.1787 derived from the plot (Fig.17 and Table 1) falls between 0 and 1, indicating that adsorption is linear and uniform over the adsorbent surface. Based on the R^2 values derived from the different isotherms tested in this work, the best-fitted adsorption isotherms were in the order of prediction precision: Langmuir > Freundlich isotherms, with corresponding R^2 values of 0.9997 and 0.9582.

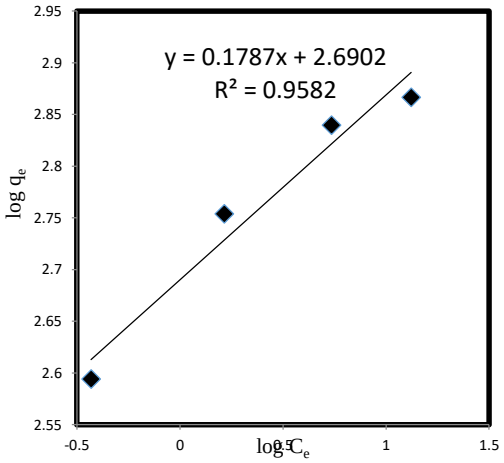

Fig. (17) Freundlich isotherm for CR adsorption on Zn-TPA-MOF.

3.2.5.2 Adsorption Isotherms of M.B. dye on Zn-TPA-MOF

Langmuir's model assumes that maximum adsorption corresponds to a saturated monolayer of M.B. dye molecules on the adsorbent surface. A linear plot (Fig.18) of specific adsorption (C_e/qe) against the equilibrium concentration ($1/Ce$) with the correlation coefficient of 0.9953 (Table 1). The calculated Langmuir monolayer adsorption capacity was found to be 147.06 mg/g. (Fig.18).

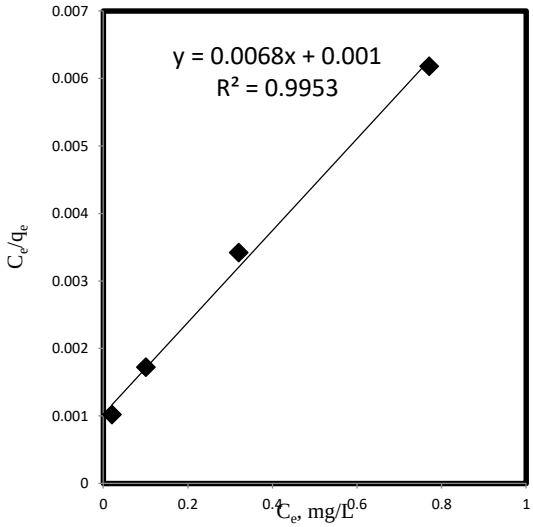

Fig.(18) Langmuir isotherm for M.B. adsorption on Zn-TPA-MOF.

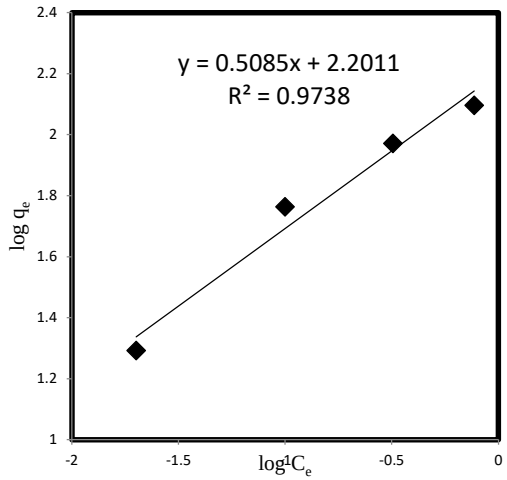

Fig.(19) Freundlich isotherm for MB adsorption on Zn-TPA-MOF.

The Freundlich model is commonly used to describe heterogeneous systems. The Freundlich parameter 1/*n* = 0.5085 obtained from the plot (Fig.19 and Table 1) falls between 0 and 1, suggesting that the adsorption is linear and uniform throughout the adsorbent surface. Based on the R^2 values obtained from various isotherms studied in this work, the best-fitted adsorption isotherms were in the order of prediction precision: Langmuir > Freundlich isotherms, and their corresponding R^2 values are 0.9953 and 0.9738. The computed 1/n values for C.R. and M.B. range between (0) and (1), indicating the simplicity of the dye adsorption process onto Zn-TPA-MOF. The values of term 1/n indicate whether the isotherm is unfavorable (1/n > 1), favorable (0 < 1/n < 1), or irreversible (1/n = 0) (Table 1).

The highest C.R. and M.B. adsorption capabilities employing Zn-TPA-MOF as an adsorbent were compared and shown in Table 2 with those of the other adsorbents previously stated. This suggests that Zn-TPA-MOF has a strong adsorption potential for both C.R. and M.B. The maximum adsorption capacity of C.R. (769.23 mg/g) and MB (147.06 mg/g) onto Zn-TPA-MOF is compared by other adsorbents (Table 2).

Table (1): Adsorption isotherm parameters of Zn-TPA-MOF obtained by fitting in Langmuir and Freundlich isotherm equations.

Dye	Langmuir adsorption			Freundlich adsorption		
	Q_m (mg/g)	b (L/mg)	R^2	log K_f	1/n	R^2
CR	769.23	2.16	0.9997	2.69	0.1787	0.9582
MB	147.06	6.80	0.9953	2.20	0.5085	0.9738

Table (2): Comparison of maximum adsorption behaviour of Zn-TPA-MOF among different adsorbents reported in literature for the adsorption of C.R. and M.B.

Adsorbent	Contact time, min.	Q_m, mg/g		Reference
		C.R.	MB	
Cu-MOF	240	828.50	–	[40]
TMU-7 (Cd)	45	97	–	[41]
Ni-MOF	300	276.7	–	[42]
TFMOF(Zr)	10	252.25	–	[43]
In-TATAB	10	299	–	[43]
Ce(III)-doped UiO-67	80	799.6	–	[44]
UiO-66	120	–	69.8	[45]
Fe_3O_4@- SiO_2@UiO-66	60	-	116	[46]
TMU-1	2880	–	100	[47]
Fe_3O_4@MIL-100(Fe)	420	–	73.8	[48]
CuBDC	20	–	41.01	[49]
USTC-1	240	–	26.6	[50]
Zn-TPA-MOF	60	769.23	147.06	***This work***

4- Conclusions

A zinc metal organic framework (Zn-TPA-MOF) was successfully created using a terephthalic solvothermal process using zinc nitrate hexahydrate salt as a starting material. The Zn-TPA-MOF structure was identified using the characterisation data. The zinc(II)-terephthalic acid metal-organic framework (Zn-TPA-MOF), which was created using a solvothermal process, was analysed using SEM/EDX, FTIR, Raman, and XRD. Raman microscopy and XRD demonstrated that terephthalic acid (TPA) acts as a bidentate ligand towards zinc(II) via the two carboxylate groups. Langmuir > Freundlich isotherms for C.R. and M.B. onto Zn-TPA-MOF were the best-fitted adsorption isotherms in order of prediction precision. Because C.R. (769.23 mg/g) and MB (147.06 mg/g) have the highest adsorption capacity, Zn-TPA-MOF has a good adsorption potential for both C.R. and MB.

5- References

1. Saravanan, A., Kumar, P.S., Yaashikaa, P.R., Karishma, S., Jeevanantham, S., Swetha, S., 2021. Mixed biosorbent of agro waste and bacterial biomass for the separation of Pb (II) ions from water system. Chemosphere 277, 130236.
2. Khan, M.I., Mubashir, M., Zaini, D., Mahnashi, M.H., Alyami, B.A., Alqarni, A.O., Show, P.L., 2021. Cumulative impact assessment of hazardous ionic liquids towards aquatic species using risk assessment methods. J. Hazard Mater. 415, 125364.
3. Murugesan, A., Loganathan, M., Senthil Kumar, P., Vo, D.V.N., 2021. Cobalt and nickel oxides supported activated carbon as an effective photocatalysts for the degradation Methylene Blue dye from aquatic environment. Sustain. Chem. Pharm. 21, 100406.
4. Renita, A.A., Vardhan, K.H., Kumar, P.S., Ngueagni, P.T., Abilarasu, A., Nath, S., Kumari, P., Saravanan, R., 2021. Effective Removal of malachite green dye from aqueous solution in hybrid system utilizing agricultural waste as particle electrodes. Chemosphere 273, 129634.
5. jtice.2015.09.002. Jiang, D., Chen, M., Wang, H., Zeng, G., Huang, D., Cheng, M., Liu, Y., Xue, W., Wang, Z. W., 2019. The application of different typological and structural MOFs-based materials for the dyes adsorption. Coord. Chem. Rev.
6. Liang, J., Ning, X. an, Sun, J., Song, J., Lu, J., Cai, H., Hong, Y., 2018. Toxicity evaluation of textile dyeing effluent and its possible relationship with chemical oxygen demand. Ecotoxicol. Environ. Saf. 166, 56–62.
7. Wong, S., Ghafar, N.A., Ngadi, N., Razmi, F.A., Inuwa, I.M., Mat, R., Amin, N.A.S., 2020. Effective Removal of anionic textile dyes using adsorbent synthesized from coffee waste. Sci. Rep. 10, 1–13.
8. Akpinar, I., Yazaydin, A.O., 2017. Rapid and efficient Removal of carbamazepine from water by UiO-67. Ind. Eng. Chem. Res. 56, 15122–15130.
9. Abhinaya, M., Parthiban, R., Kumar, P.S., Vo, D.V.N., 2021. A review on cleaner strategies for extraction of chitosan and its application in toxic pollutant removal. Environ. Res. 196, 110996.
10. Sharma, G., AlGarni, T.S., Kumar, P.S., Bhogal, S., Kumar, A., Sharma, S., Naushad, M., ALOthman, Z.A., Stadler, F.J., 2021. Utilization of Ag_2O–Al_2O_3–ZrO_2 decorated onto rGO as adsorbent for the Removal of Congo red from aqueous solution. Environ. Res. 197, 111179.
11. Ullah, S., Al-Sehemi, A.G., Mubashir, M., Mukhtar, A., Saqib, S., Bustam, M.A., Cheng, C. K., Ibrahim, M., Show, P.L., 2021. Adsorption behavior of mercury over hydrated lime: experimental investigation and adsorption process characteristic study. Chemosphere 271, 129504.
12. Li, C.P., Zhou, H., Chen, J., Wang, J.J., Du, M., Zhou, W., 2020. A highly efficient coordination polymer for selective trapping and sensing of perrhenate/ pertechnetate. ACS Appl. Mater. Interfaces 12, 15246–15254.
13. Zou, K.Y., Li, Z.X., 2018. Controllable syntheses of MOF-derived materials. Chem. Eur J. 24, 6506 - 6518
14. Guo, Z., Zhang, Z., Li, Z., Dou, M., Wang, F., 2019. Well-defined gradient Fe/Zn bimetal organic framework cylinders derived highly efficient iron- and nitrogen- codoped hierarchically porous carbon electrocatalysts towards oxygen reduction. Nanomater. Energy 57, 108–117.
15. Kang, Y.S., Lu, Y., Chen, K., Zhao, Y., Wang, P., Sun, W.Y., 2019. Metal–organic frameworks with catalytic centers: from synthesis to catalytic application. Coord. Chem. Rev. 378, 262–280.
16. Nivetha, R., Kollu, P., Chandar, K., Pitchaimuthu, S., Jeong, S.K., Grace, A.N., 2019. Role of MIL-53(Fe)/hydrated-dehydrated MOF catalyst for electrochemical hydrogen evolution reaction (HER) in alkaline medium and photocatalysis. RSC Adv. 9, 3215–3223.
17. Guo, Z., Zhang, Z., Li, Z., Dou, M., Wang, F., 2019. Well-defined gradient Fe/Zn bimetal organic framework cylinders derived highly efficient iron- and nitrogen- codoped hierarchically porous carbon electrocatalysts

towards oxygen reduction. Nanomater. Energy 57, 108–117.
18. Kim, D., Lee, G., Oh, S., Oh, M., 2019. Unbalanced MOF-on-MOF growth for the production of a lopsided core-shell of MIL-88B@MIL-88A with mismatched cell parameters. Chem. Commun. 55, 43–46.
19. Lin, S., Zhao, Y., Yun, Y.S., 2018. Highly effective removal of nonsteroidal anti-inflammatory pharmaceuticals from water by Zr(IV)-Based metal-organic framework: adsorption performance and mechanisms. ACS Appl. Mater. Interfaces 10, 28076–28085.
20. Hermes, S., Schr¨oder, F., Chelmowski, R., W¨oll, C., Fischer, R.A., 2005. Selective nucleation and growth of metal organic open framework thin films on patterned COOH/CF3-terminated self-assembled monolayers on Au (111). J. Am. Chem. Soc. 127, 13744–13745.
21. Khan, N.A., Yoo, D.K., Jhung, S.H., 2018. Polyaniline-Encapsulated metal-organic framework MIL-101: adsorbent with record-high adsorption capacity for the Removal of both basic quinoline and neutral indole from liquid fuel. ACS Appl. Mater. Interfaces 10, 35639–35646.
22. Yu, S., Jiang, Z., Li, W., Mayta, J.Q., Ding, H., Song, Y., Li, Z., Dong, Z., Pan, F., Wang, B., Zhang, P., Cao, X., 2018. Elevated performance of hybrid membranes by incorporating metal organic framework CuBTC for pervaporative desulfurization of gasoline. Chem. Eng. Process. Process Intensif. 123, 12–19.
23. Zhang, Y., Jiang, Z., Song, Jing, Song, Jian, Pan, F., Zhang, P., Cao, X., 2019. Elevated pervaporative desulfurization performance of pebax-Ag+@MOFs hybrid membranes by integrating multiple transport mechanisms. Ind. Eng. Chem. Res. 58, 16911–16921.
24. Liu, G., Tian, M., Lu, M., Shi, W., Li, L., Gao, Y., Li, T., Xu, D., 2021. Preparation of magnetic MOFs for use as a solid-phase extraction absorbent for rapid adsorption of triazole pesticide residues in fruits juices and vegetables. J. Chromatogr. B Anal. Technol. Biomed. Life Sci. 1166, 122500.
25. Rocío-Bautista, P., Termopoli, V., 2019. Metal–Organic Frameworks in Solid-phase Extraction Procedures for Environmental and Food Analyses. Chromatographia.
26. Gonz'alez-Hern'andez, P., Pacheco-Fern'andez, I., Bernardo, F., Homem, V., Pas'an, J., Ayala, J.H., Ratola, N., Pino, V., 2021. Headspace solid-phase microextraction based on the metal-organic framework CIM-80(Al) coating to determine volatile methylsiloxanes and musk fragrances in water samples using gas chromatography and mass spectrometry. Talanta 232, 122440.
27. Zhang, Q.C., Xia, G.P., Liang, J.Y., Zhang, X.L., Jiang, L., Zheng, Y.G., Wang, X.Y., 2020. NH2-MIL-53(Al) polymer monolithic column for in-tube solid-phase microextraction combined with UHPLC-MS/MS for detection of trace sulfonamides in food samples. Molecules 25.
28. Aqel, A., Alkatheri, N., Ghfar, A., Alsubhi, A.M., ALOthman, Z.A., Badjah-Hadj- Ahmed, A.Y., 2021. Preparation of value-added metal-organic frameworks for high-performance liquid chromatography. Towards green chromatographic columns. J. Chromatogr. A 1638, 461857.
29. Nguyen, Tien, 2019. Versatile MOF separates drug molecule enantiomers. C&EN Glob. Enterp. 97, 9.
30. Sohrabi, M.R., Matbouie, Z., Asgharinezhad, A.A., Dehghani, A., 2013. Solid phase extraction of Cd (II) and Pb (II) using a magnetic metal-organic framework, and their determination by FAAS. Microchim. Acta 180, 589–597.
31. Chen, W., et al., Synthesis and luminescence properties of brick-shaped lanthanum–organic frameworks with mesoporous and macroporous architectures. Luminescence, 2017. 32(7): p. 1289-1293.
32. Ponnusamy, S.K. and Subramaniam, R. 2013. Process optimization studies of Congo red dye adsorption onto cashew nut shell using response surface methodology. International Journal of Industrial Chemistry, 4(1): p. 1-10.
33. Amar, I.A., et al., 2021. Adsorptive Removal of congo red dye from aqueous solutions using Mo-doped $CoFe_2O_4$ magnetic nanoparticles. Pigment & Resin Technology.
34. Ahmed, D.N., et al., 2020. Waste foundry sand/MgFe-layered double hydroxides composite material for efficient Removal of Congo red dye from aqueous solution. Scientific reports, 10(1): p. 1-12.
35. Ghasemzadeh, M.A., Abdollahi-Basir, M.H., Mirhosseini-Eshkevari, B. 2018. Multi-component synthesis of spiro[diindeno[1,2-b:20,10 -e]pyridine-11,30 -indoline]- triones using zinc terephthalate metal-organic frameworks, Green Chem. Lett. Rev. 11 (1) 47–53,
36. Bordiga, S., Lamberti, C., Ricchiardi, G., Regli, L., Bonino, F., Damin, A., Lillerud, K.P., Bjorgen, M., Zecchina, A. 2004. Chem. Commun. 2300–2301.

37. Hu, Y.H., Zhang, L. 2010. Amorphization of metal-organic framework MOF-5 at unusually low applied pressure, Phys. Rev. B 81, 174103
38. Langmuir, I. 1918. The adsorption of gases on plane surfaces of glass, mica and platinum, J. Am. Chem. Soc., 40, 1361–1403.
39. Freundlich, H. 1906. Adsorption in solution, Phys. Chem. Soc., 40, 1361–368.
40. Hu, J., Yu, H., Dai, W., Yan, X., Hu, X., Huang, H., 2014. Enhanced adsorptive Removal of hazardous anionic dye "Congo red" by a Ni/Cu mixed-component metal-organic porous material. RSC Adv. 4, 35124–35130.
41. Masoomi, M.Y., Bagheri, M., Morsali, A., 2017. Porosity and dye adsorption enhancement by ultrasonic synthesized Cd(II) based metal-organic framework. Ultrason. Sonochem. 37, 244–250.
42. Yang, M., Bai, Q., 2019. Flower-like hierarchical Ni-Zn MOF microspheres: efficient adsorbents for dye removal. Colloids Surfaces A Physicochem. Eng. Asp. 582, 123795.
43. Liu, J., Yu, H., Wang, L., 2020. Superior absorption capacity of tremella like ferrocene based metal-organic framework in Removal of organic dye from water. J. Hazard Mater. 392, 122274.
44. Yang, H., He, X.W., Wang, F., Kang, Y., Zhang, J., 2012. Doping copper into ZIF-67 for enhancing gas uptake capacity and visible-light-driven photocatalytic degradation of organic dye. J. Mater. Chem. 22, 21849–21851.
45. Molavi, H., Hakimian, A., Shojaei, A., Raeiszadeh, M., 2018. Selective dye adsorption by highly water stable metal-organic framework: long term stability analysis in aqueous media. Appl. Surf. Sci. 445, 424–436.
46. Huang, L., He, M., Chen, B., Hu, B., 2018. Magnetic Zr-MOFs nanocomposites for rapid Removal of heavy metal ions and dyes from water. Chemosphere 199, 435–444.
47. Hu, M.L., Hashemi, L., Morsali, A., 2016. Pore size and interactions effect on Removal of dyes with two lead(II) metal-organic frameworks. Mater. Lett. 175, 1–4.
48. Shao, Y., Zhou, L., Bao, C., Ma, J., Liu, M., Wang, F., 2016. Magnetic responsive metal – organic frameworks nanosphere with core – shell structure for highly efficient Removal of methylene blue. Chem. Eng. J. 283, 1127–1136.
49. Doan, V.D., Do, T.L., Ho, T.M.T., Le, V.T., Nguyen, H.T., 2020. Utilization of waste plastic pet bottles to prepare copper-1,4-benzenedicarboxylate metal-organic framework for methylene blue removal. Separ. Sci. Technol. 55, 444–455.
50. Li, B., Jiang, W., Xu, Y., Xu, Z., Yan, Q., Yong, G., 2020. Dyes encapsulated in a novel flexible metal-organic framework show tunable and stimuli-responsive phosphorescence. Dyes Pigments 174.